Symposium on Optical Fiber Measurements, (SOFM 2000), Sep 26-28, 2000, Boulder, CO, NIST Special Publication 953, pp. 169-172

A fast and accurate measurement of both transmission and reflection group delay in fiber Bragg gratings

Shellee D. Dyer and Kent B. Rochford
National Institute of Standards and Technology
Optoelectronics Division
325 Broadway, Boulder, CO 80303

We show that both the reflection and transmission group delay of fiber Bragg gratings can be accurately obtained from one low-coherence interferometric measurement. The spectral reflectance and transmittance of the grating can also be obtained from that same measurement. Both the reflection and transmission group delay can be obtained in less than 60 seconds. This technique can also be applied to the simultaneous measurement of the group delay of multiple fiber Bragg gratings in series.

1. Introduction

Low-coherence interferometry has several advantages over conventional techniques such as the modulation-phase shift method [1] for the characterization of fiber Bragg gratings (FBGs). A key advantage is the rapidity with which a measurement of group delay and reflectance can be obtained. The interferogram is obtained in less than a second, and processing the interferogram to obtain group delay or reflectance takes less than 60 seconds [2], compared with the conventional modulation-phase shift measurement, which can take several hours [1].

This measurement technique has low uncertainty (less than 1.5 ps) and, because of its speed, is immune to errors caused by thermal variations and instrument drift. Low-coherence interferometry is also immune to the ripple washout problems that can occur with the modulation-phase shift measurement [3].

2. Measurement Method

A diagram of the low-coherence interferometric system is shown in Fig. 1. A broadband Er superfluorescent fiber source (SFS) provides the input signal. This source is directed into a pair of fiber couplers. Fiber coupler 1 provides a comparison signal for the difference-over-sum (Δ/Σ) amplifier, as explained below. Fiber coupler 2 is part of a fiber-optic Michelson interferometer. The

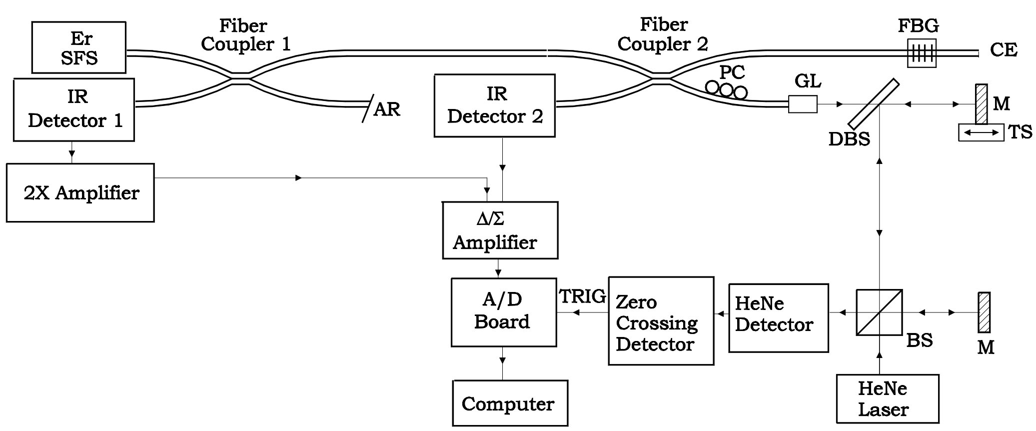

Figure 1. Diagram of low-coherence interferometric system for measurement of the transmission and reflection group delay of FBGs. AR: anti-reflection coating, PC: polarization controller, GL: grin lens, CE: cleaved endface, M: mirror, TS: translation stage, BS: beamsplitter, DBS: dichroic beamsplitter, Δ/Σ: difference over sum.

FBG under test is spliced onto the test arm of the interferometer. The far end of the grating's fiber pigtail is cleaved to produce a Fresnel reflection. This reflection facilitates the measurement of transmission group delay, as explained below.

The reference arm of the interferometer contains a variable-length air path so that the total optical path difference (OPD) of the interferometer can be varied. A frequency-stabilized HeNe laser interferometer monitors the position of the reference arm mirror, and a zero-crossing detector triggers sampling of the IR signal on positive-sloped zero crossings of the HeNe signal.

The light from the reference arm is recombined with the light from the test arm at fiber coupler 2, and the recombined light is directed onto the two IR detectors. The signals at the two IR detectors have similar source excess-noise characteristics, while the interference terms are 180° out of phase. Therefore, using a difference-over-sum amplifier will reduce excess noise from the SFS, which is the dominant noise source. This improves the interferogram's signal-to-noise ratio (SNR) by a factor of 3, and yields a corresponding improvement in the group delay SNR.

If the spacing between the FBG and the cleaved endface exceeds the width of the individual coherence functions, then the signal at the detector as a function of the OPD consists of two distinct signatures. One of these signatures represents the interference of light reflected from the FBG with the light reflected from the reference arm mirror. The other signature is created by the interference of light reflected from the test arm's cleaved endface with the light from the reference arm.

The shape and extent of the first signature is determined by the reflection characteristics of the FBG. Neglecting background dispersion, the complex degree of coherence $\gamma(\xi)$ of this interferogram is given by [4]

$$\gamma(\xi) = \int_{-\infty}^{\infty} G(\sigma) r(\sigma) \exp(j\phi_r(\sigma)) \exp(j2\pi\sigma\xi) d\sigma \,, \tag{1}$$

where ξ is the OPD, σ is the wavenumber, $G(\sigma)$ is the power spectral density of the Er SFS, and $r(\sigma)\exp(j\phi_r(\sigma))$ is the complex field reflection coefficient of the FBG. The reflection group delay (t_g) of this grating is calculated from the phase of the Fourier transform of the interferogram as follows:

$$t_g = \frac{1}{2\pi c} \frac{d}{d\sigma} \phi_r(\sigma) \,. \tag{2}$$

Similarly, the second interferogram is related to the complex field transmission coefficient of the FBG as follows:

$$\gamma(\xi) = \int_{-\infty}^{\infty} G(\sigma) \left[t(\sigma) \exp(j\phi_t(\sigma)) \right]^2 \exp(j2\pi\sigma\xi) d\sigma \,, \tag{3}$$

where $t(\sigma)\exp(j\phi_t(\sigma))$ is the complex field transmission coefficient of the FBG. The equations above are derived assuming that the only dispersion difference between the two arms arises from the dispersion of the FBG. In reality, there is a small background dispersion from the difference in the length of the test and reference arm fibers, but the slope of the background group delay is approximately 11 fs/nm, which is negligible compared with the dispersion of a typical FBG [5].

3. Data Processing

The reflection group delay was calculated from the FBG reflection interferogram. We truncated the interferogram at the points where the SNR was approximately unity. Next, we appended zeros to the interferogram array (zero padding) to obtain a total array length of 2^N. The choice of N determines the wavelength resolution of the group delay results. Larger values of N give better resolution, but if N is too large, computational errors such as roundoff error affect the accuracy of the results. For the results shown in this paper, we used N=18, giving a wavelength resolution of 14 pm.

To obtain the group delay, we took the Fourier transform of the truncated and padded interferogram. The magnitude of the Fourier transform is proportional to the magnitude of the field reflection coefficient of the FBG. The relative group delay of the FBG is determined by differentiating the phase of the Fourier transform.

The transmission group delay is calculated from the cleaved endface interferogram in a manner similar to the calculation of the reflection group delay. We truncate and zero pad the interferogram, take the Fourier transform, and then calculate group delay by differentiating the phase of the Fourier transform.

4. Experimental Results

We used our interferometric measurement system to determine the transmission and reflection group delay of a chirped FBG with a 5.4 nm bandwidth and a center wavelength of 1555.5 nm (grating A). We cleaved the end of the FBG fiber at a distance of approximately 2.7 cm from the grating. We then measured the interference pattern as a function of OPD and obtained two distinct signatures. From the second interferogram, we calculated the double-pass transmission group delay of this grating, which is shown in Fig. 2. Also shown in Fig. 2 is the relative power transmitted by the grating. The transmission group delay results are valid only in regions where the transmitted power is appreciable; in all other spectral regions there is insufficient signal for an accurate measurement. From Fig. 2, we see that the transmission group delay of this grating has features that extend beyond the 10dB reflection bandwidth of the grating.

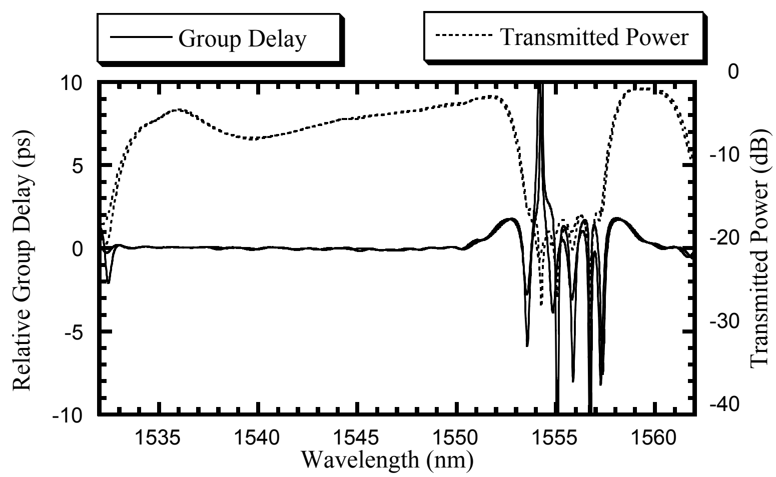

Figure 2. Double-pass transmission group delay and relative transmitted power of grating A. Results are shown from two repeated measurements.

We also used our interferometric system to measure the group delay of two gratings in series. We spliced a second grating approximately 6.5 cm after grating A. This second grating (grating B) had a center wavelength of 1548 nm and a 1.7 nm bandwidth. The endface of the test arm was immersed in index matching fluid; therefore, the interferometer output consisted of two separate interferograms, one for each of the two gratings. The shape of the interferogram from grating A's reflection is determined by the complex field reflection coefficient of that grating as given by Eq. 1. The light transmitted by grating A sees the effects of both gratings, and that interferogram is related to both gratings as follows:

$$\gamma(\xi) = \int_{-\infty}^{\infty} G(\sigma)[t_A(\sigma)\exp(j\phi_{tA}(\sigma))]^2 r_B(\sigma)\exp(j\phi_{rB}(\sigma))\exp(j2\pi\sigma\xi)d\sigma\,, \qquad (4)$$

where $t_A(\sigma)\exp(j\phi_{tA}(\sigma))$ is the complex field transmission coefficient of grating A, and $r_B(\sigma)\exp(j\phi_{rB}(\sigma))$ is the complex field reflection coefficient of grating B. We processed each interferogram separately by truncating each near the points where the SNR was equal to one. We then zero padded each interferogram to create arrays of length 2^{18} and calculated the Fourier transform of each padded interferogram. From the phase of the Fourier transform of grating A's interferogram, we obtained the reflection group delay of that grating, which is shown in Fig. 3. From the second interferogram, we obtained a group delay function, also shown in Fig. 3, which is the product of the reflection group delay of grating B with the double-pass transmission group delay of grating A. These results are relative group delay curves, and therefore each curve has its own arbitrary additive constant; the relative group delay difference between the gratings is not shown in this graph. Comparing this group delay product at wavelengths near 1548 nm with the transmission group delay of the grating A shown in Fig. 2, it is clear that the transmission group delay of grating A is very small at wavelengths near 1548 nm, and can be neglected compared with the reflection group delay of grating B.

We also measured the group delay difference arising from the fiber separation between the two gratings. To obtain this, we calculated the central fringe index of each individual interferogram [6]. Then we determined the group delay difference from the separation between the interferograms' central fringes. We calculated a total single-pass delay between the gratings of 315 ps, which is too large to show in Fig. 3.

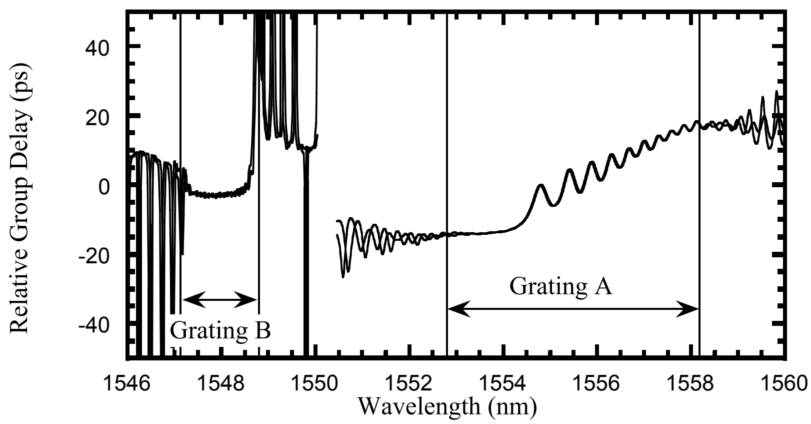

Figure 3. Plot of relative reflection group delay measured of two gratings in series. Results are shown from two repeated measurements. The relative group delay difference between the two gratings is not shown.

5. Conclusions

We have demonstrated the measurement of transmission group delay in FBGs, as well as the measurement of the group delay of multiple gratings in series using low-coherence interferometry. The key advantage of the low-coherence technique is speed, and it is possible to obtain the group delay measurements in less than 60 seconds.

References

[1] S.E. Mechels, J.B. Schlager, and D.L. Franzen, "Accurate measurements of the zero-dispersion wavelength in optical fibers," *J. Res. Natl. Inst. Stand. Technol*., vol. 102, pp. 333-347, 1997.

[2] S.D. Dyer, K.B. Rochford, and A.H. Rose, "Fast and accurate low-coherence interferometric measurements of fiber Bragg grating dispersion and reflectance," *Optics Express*, vol. 5, pp. 262-266, 1999.

[3] R.M. Fortenberry, "Enhanced wavelength resolution chromatic dispersion measurements using fixed sideband technique," in *Optical Fiber Communications Conference*, OSA Technical Digest (Optical Society of America, Washington DC, 2000), TuG8, pp. 107-109.

[4] U. Wiedmann, P. Gallion, and G.-H. Duan, "A generalized approach to optical low-coherence reflectometry including spectral filtering effects," *Journal of Lightwave Technology*, vol. 16, pp. 1343-1347, 1998.

[5] S.D Dyer and K.B. Rochford, "Low-coherence interferometric measurements of fibre Bragg grating dispersion," *Electronics Letters*, vol. 35, pp. 1485-1486, 1999.

[6] B.L. Danielson and C.Y. Boisrobert, "Absolute optical ranging using low-coherence interferometry," *Applied Optics*, vol. 30, pp. 2975-2979, 1991.